Paper accepted for presentation at 2009 IEEE Bucharest Power Tech Conference, June 28th - July 2nd, Bucharest, Romania

Impact of SSSC on the Digital Distance Relaying

A. Salemnia, M. Khederzadeh, *Senior Member, IEEE,* and A. Ghorbani

***Abstract*—This paper presents analytical and simulation results of the application of distance relays for the protection of transmission employing Static Synchronous Series Compensator (SSSC). Firstly a detailed model of the SSSC and its control is proposed and then the situation is studied analytically, where the errors introduced in the impedance measurement due to the presence of SSSC on the line are analyzed. The simulation results show the impact of SSSC on the performance of a distance protection relay for different fault conditions; the studies also include the influence of the operational mode of SSSC and its location on the transmission system. The complete digital simulation study using the full 48-pulse GTO-SSSC model. The digital simulation is performed in the MATLAB/Simulink software environment using the Power System Blockset (PSB).**

***Index Terms*— Flexible AC Transmission Systems (FACTS), Static Synchronous Series Compensator (SSSC), Distance relay.**

I. INTRODUCTION

THE use of power electronics devices to improve power transfer capability of long transmission lines forms the basis of the concept of FACTS. The Static Synchronous Series Compensator (SSSC) is a series device of the FACTS family using power electronics to control power flow and improve power oscillation damping on power grids. The SSSC is a static synchronous generator operated without an external electric energy source as a series compensator whose output voltage is in quadrature with, and controllable independently of, the line current for the purpose of increasing or decreasing the overall reactive voltage drop across the line and thereby controlling the transmitted electric power [1]. When an SSSC injects an alternating voltage leading the line current, it emulates an inductive reactance in series with the transmission line causing the power flow as well as the line current to decrease as the level of compensation increases and the SSSC is considered to be operating in an inductive mode. When an SSSC injects an alternating voltage lagging the line current, it emulates a capacitive reactance in series with the transmission line causing the power flow as well as the line current to increase as the level of compensation increases and the SSSC is considered to be operating in a capacitive mode [2] therefore SSSC apply rapid changes in system parameters such as line impedance and line currents. Distance protection relays have been widely applied for protecting transmission lines. The operating principle of distance protection is based on the fact that, from any measuring point in power system the line impedance to a fault in that system can be determined by measuring the voltage and current at the measuring point [3].

The presence of a SSSC in the fault loop affects both the steady state and transient components in the voltage and current. Therefore, the apparent impedance calculations should take into account the variable series voltage source or the SSSC. The apparent impedance seen by a distance relay is influenced greatly by the location and operational mode of SSSC.

Some research has been done to evaluate the performance of a distance relay for transmission systems with FACTS controllers. The work in [4] has presented analytical and simulation results for investigating the operation of impedance-based protection relays in a power system containing a STATCOM and the analyses are based on steady-state operation for modeling the STATCOM and the protection relays. The work in [5], presents a study of the performance of distance protection relays when applied to protect shunt FACTS compensated transmission lines and effect of two types of shunt FACTS devices, SVC and STATCOM are studied. In [6], the voltage-source model of FACTS controllers has been employed to study the impact of FACTS on the tripping boundaries of distance relay. The work in [7] shows a comprehensive analysis of the impact of TCSC on the protection of transmission lines and shows that not only the TCSC affects the protection of its line, but also the protection of adjacent lines would experience problems. The studies in [8], also shows that the presence of FACTS controllers in a transmission line will affect the trip boundary of a distance relay, and both the parameters of FACTS controllers and their location in the line have an impact on the trip boundary. There has been considerable work to study the effect of series compensation including series FACTS devices on the performance of distance protection relays [9], [10]. In [11], an apparent impedance calculation procedure for a transmission line with UPFC based on the power frequency sequence component is then investigated and studies also include the influence of the setting of UPFC control parameters and the operational mode of UPFC.

The outline of this paper is as follows: Section II describes the SSSC and transmission system model. The apparent impedance calculation is presented in section III. Section IV

A. Salemnia and M. Khederzadeh are Assistant Professors in Electrical Department Engineering of Power and Water University of Technology, Tehran, Iran.(e-mail: Salemnia@pwut.ac.ir, Khederzadeh@pwut.ac.ir)

A. Ghorbani is M.Sc. student in Power and Water University of Technology, Tehran, Iran.(e-mail: amirghorbani@stud.pwut.ac.ir)

978-1-4244-2235-7/09/$25.00 ©2009 IEEE

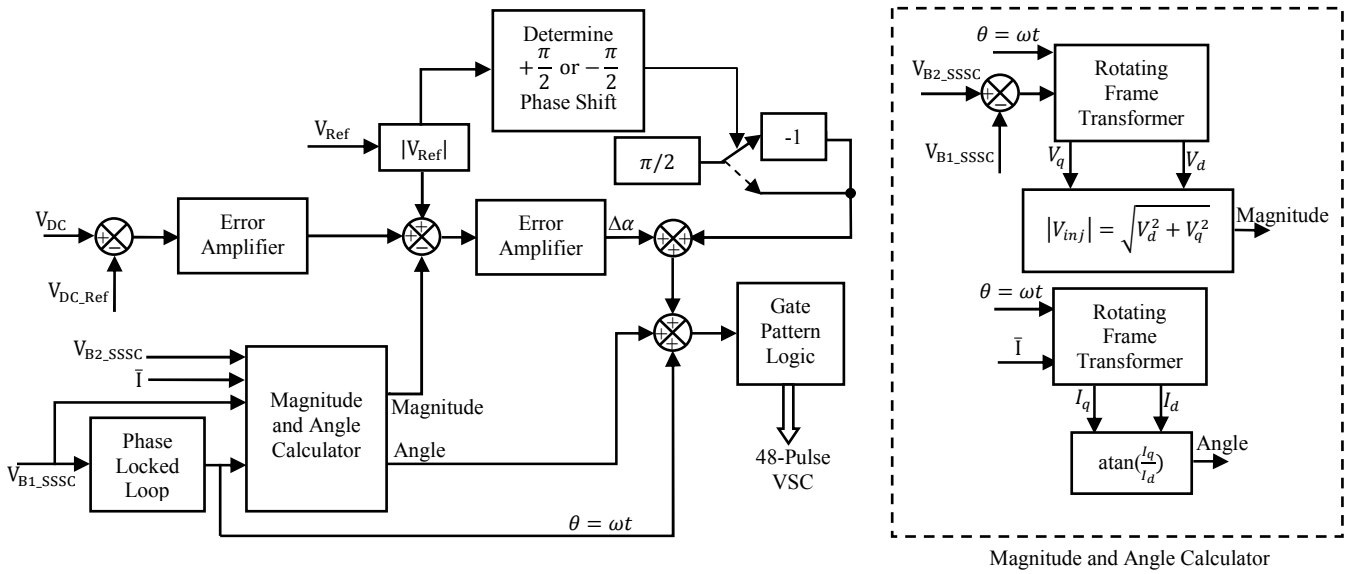

Fig. 1. Control block diagram of a SSSC

describes the relay modelling and simulation results are presented in section V.

II. SSSSC and Transmission System Model

A. Power System Description

A double circuit transmission line connecting two sources possessing a 100-MVA SSSC in one of its circuits at midpoint. Modeling the unified ac grid sample system with the SSSC is done using MATLAB/Simulink as shown in Fig. 2. Two 200-km parallel 500-kV transmission lines terminated in two sources are considered with the angle difference of 20 degrees.

B. Modeling of SSSC

The series reactive compensation scheme, using a switching power converter (voltage-sourced converter) as a synchronous voltage source to produce a controllable voltage in quadrature with the line current as defined by (1).

$$\overline{V_{inj}} = |X_q|\bar{I}e^{\pm j90^\circ} \quad (1)$$

The SSSC is able to maintain a constant compensating voltage in the presence of variable line current, or control the amplitude of the injected compensating voltage independent of the amplitude of the line current. For normal capacitive compensation, the output voltage lags the line current by 90 degrees. For SSSC, the output voltage can be reversed by simple control action to make it lead or lag the line current by 90 degrees. In this case, the injected voltage decreases the voltage across the inductance line impedance and thus the series compensation has the same effect as if the reactance line impedance was increased [1]. Fig. 2(a) shows an SSSC connected in series with a simple transmission line between B1 and B2. The SSSC is modeled by a series connected voltage source in series with an impedance. This impedance represents the impedance of coupling transformer.

The voltage source converter described in this paper is a harmonic neutralized, 48-pulse GTO converter. It consists of four three-phase, three-level inverters and four phase-shifting transformers. In the 48-pulse voltage source converter, the dc bus V_{dc} is connected to the four three-phase inverters. The four voltage generated by the inverters are applied to secondary windings of four zig-zag phase-shifting transformers connected in Y or Δ [12].

Fig. 1 shows the control block diagram of an SSSC. An instantaneous 3-phase set of line voltages, at B1 is used to calculate the reference angle $\theta = \omega t$ and is decomposed into its real or direct component, V_d and reactive or quadrature component, V_q and then the amplitude, V_{inj} is calculated. The compensating voltage, V_{inj} is controlled by a simple closed loop: the absolute value of reference, V_{Ref} is compared to the measured magnitude of the injected voltage, V_{inj} and the amplified difference (error) is passed through a PI controller (Error Amplifier) and then is added, as a correction angle $\Delta\alpha$, to the synchronizing signal $\theta = \omega t$. An instantaneous 3-phase set of measured line currents, I is decomposed into its real or direct component, I_d and reactive or quadrature component, I_q and then the relative angle, of the line current with respect to the phase-lock-loop angle, are calculated. The phase shifter is operated from the output of polarity detector which determines whether reference, V_{Ref} is positive (capacitive) or negative (inductive). Depending on the polarity of $\Delta\alpha$, angle θ and consequently the converter gate drive signals will be advanced or retarded and, thereby the compensating voltage, V_{inj} will be shifted with respect to the prevailing line current from its original +π/2 or -π/2 phase position. This phase shift will cause the converter to absorb real power from the ac system for the dc capacitor or, vice versa supple that to the ac system from the dc capacitor. As a result, the voltage of the dc capacitor will increase or decrease, causing a corresponding change in the magnitude of the compensating voltage. Once the desired magnitude of V_{inj} is reached the substantially quadrature relationship between the line current and compensating voltage gets reestablished with only a remaining

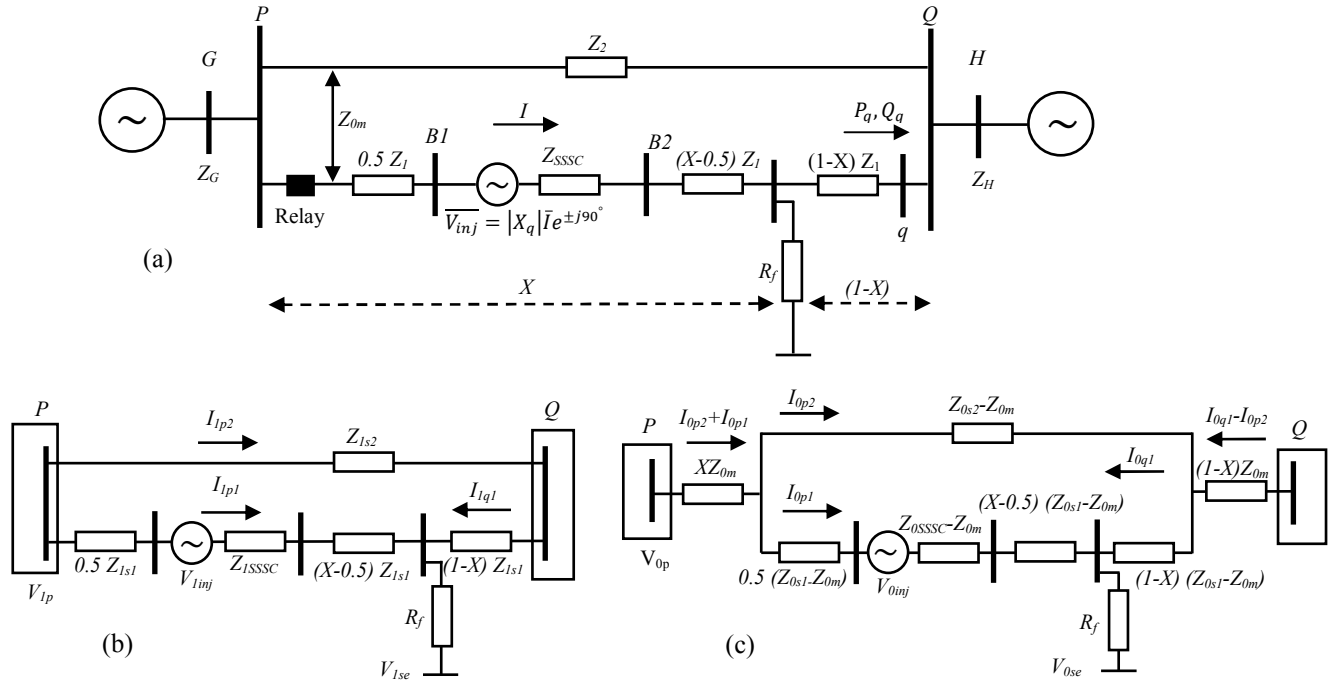

Fig. 2. (a) Transmission system with equivalent circuit of SSSC; (b) positive sequence network; (c) zero sequence network.

small, steady angular difference necessary to absorb power from the ac system to replenish the operating losses of the converter [1], [2].

Fig. 3 shows the digital simulation results when an SSSC emulates a reactance in series with the transmission line. At 0.15 s, an inductive reactance compensation of 0.07 per unit is requested. The inverter output 48-pulse voltage, V_{inja}, of phase a leads the line current, I_a, by almost 90°. As the inductive reactance demand increases, the line current, I_a, and the power flow, P_q, and Q_q, in the transmission line decrease. At 0.31 s, a capacitive reactance compensation of 0.1 per unit is requested. The inverter voltage, V_{inja}, lags the line current, I_a, by almost 90°. As the capacitive reactance demand increases, the line current, I_a, and the power flow, P_q, and Q_q, in the transmission line increase. It can also be observed that the SSSC has, as expected, an excellent (subcycle) response time. Fig. 4 shows the expanded view of the two sections of Fig. 3. The inverter voltage shows the presence of 48-pulse harmonic components.

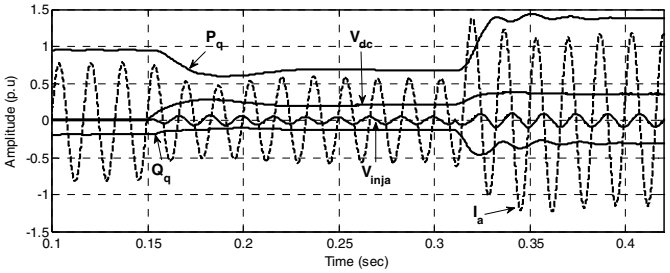

Fig. 3. Performance of a SSSC with a 48-Pulse harmonic neutralized inverter operating in inductive and capacitive modes.

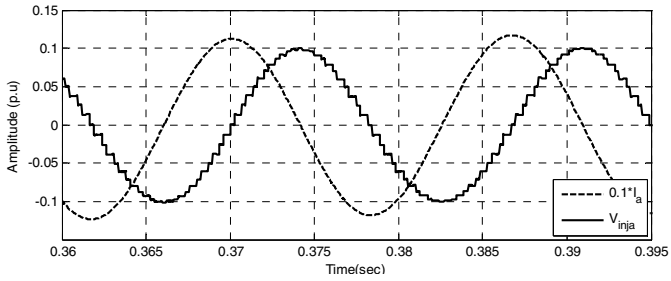

Fig. 4. 48-pulse converter output voltage and line current.

III. Apparent Impedance Calculation

A double-circuit transmission line fed from both ends with SSSC installed in the middle of the second transmission line subjected to a single line to ground fault as shown in Fig. 2 (a) is considered. When a single phase-to-ground fault occurs on the right side of the SSSC and the distance is X from the relay point, the positive (negative sequence network is similar with positive sequence network) and zero sequence networks of the system during the fault are as shown respectively in Fig. 2(b) and (c). For convenience, the following nomenclature are defined:

V_p: is phase voltage at relay location at bus P;

I_{p1}: is phase current through faulty line at relay location at bus P;

I_{p2}: is phase current through sound line at relay location at bus P;

V_{0p}, V_{1p}, V_{2p}: are sequence phase voltages at relay location at bus P;

I_{0p1}, I_{1p1}, I_{2p1}: are sequence phase currents through faulty line at relay location at bus P;

I_{0p2}, I_{1p2}, I_{2p2}: are sequence phase currents through sound line at relay location at bus P;

I_{0q1}, I_{1q1}, I_{2q1}: are sequence phase currents through faulty line at bus Q;
V_{0se}, V_{1se}, V_{2se}: are sequence phase voltages at fault location E;
R_f : is fault resistance;
Z_{0s1}, Z_{1s1}, Z_{2s1}: are sequence impedances of the faulty line and Z_{1s1}=Z_{2s1}.
Z_{0s2}, Z_{1s2}, Z_{2s2}: are sequence impedances of the sound line and Z_{1s2}=Z_{2s2}.
Z_{0m}: is the zero sequence mutual impedance between the faulty and sound lines.
Z_{0G}, Z_{1G}, Z_{2G}, Z_{0H}, Z_{1H}, Z_{2H}: are sequence impedance of generators G and H respectively [13].

A. SSSC at the Midpoint

By using data of the faulty and sound lines at bus P, the following equations can be derived:

$$\begin{cases} V_{1p} = xZ_{1s1}I_{1p1} + R_f(I_{1p1} + I_{1q1}) + Z_{1SSSC}I_{1p1} \\ \qquad +V_{1inj} + V_{1se} \qquad (a) \\ V_{1p} = Z_{1s2}I_{1p2} + (1-x)Z_{1s1}I_{1q1} + R_f(I_{1p1} + I_{1q1}) \\ \qquad +V_{1se} \qquad (b) \end{cases} \tag{2}$$

By eliminating the term V_{1se}, from 2(a) and 2(b), the following equation is obtained:

$$I_{1q1} = \frac{xI_{1p1} - k_1 I_{1p2}}{1-x} + \frac{V_{1inj}}{(1-x)Z_{1s1}} + \frac{Z_{1SSSC}I_{1p1}}{(1-x)Z_{1s1}} \tag{3}$$

Where: $k_1 = Z_{1s2}/Z_{1s1}$ (4)

By substituting (3), in 2(a), the following equation is obtained:

$$V_{1p} = V_{1se} + I_{1p1}\left(xZ_{1s1} + \frac{AZ_{1SSSC}}{(1-x)Z_{1s1}}\right) + \frac{R_f}{(1-x)}\left(I_{1p1} - k_1 I_{1p2}\right) + \frac{AV_{1inj}}{(1-x)Z_{1s1}} \tag{5}$$

Where: $A = (1-x)Z_{1s1} + R_f$ (6)

For negative sequence:

$$\begin{cases} V_{2p} = xZ_{1s1}I_{2p1} + R_f(I_{2p1} + I_{2q1}) + Z_{1SSSC}I_{2p1} \\ \qquad +V_{2inj} + V_{2se} \qquad (a) \\ V_{2p} = Z_{1s2}I_{2p2} + (1-x)Z_{1s1}I_{2q1} + R_f(I_{2p1} + I_{2q1}) \\ \qquad +V_{2se} \qquad (b) \end{cases} \tag{7}$$

By eliminating terms containing I_{2q1}, from 7(a) and 7(b), the following is obtained:

$$V_{2p} = V_{2se} + I_{2p1}\left(xZ_{1s1} + \frac{AZ_{1SSSC}}{(1-x)Z_{1s1}}\right) + \frac{R_f}{(1-x)}\left(I_{2p1} - k_1 I_{2p2}\right) + \frac{AV_{2inj}}{(1-x)Z_{1s1}} \tag{8}$$

For zero sequence:

$$\begin{cases} V_{0p} = x\left(Z_{0m}I_{0p2} + Z_{0s1}I_{0p1}\right) + R_f(I_{0p1} + I_{0q1}) \\ +Z_{0SSSC}I_{0p1} + V_{0q} + V_{0se} \qquad (a) \\ V_{0p} = xZ_{0m}\left(I_{0p2} + I_{0p1}\right) + (Z_{0s2} + Z_{om})I_{0p2} \\ +(Z_{0s1} - Z_{om})(1-x)I_{0q1} + R_f(I_{0p1} + I_{0q1}) + V_{0se} \qquad (b) \end{cases} \tag{9}$$

By eliminating terms containing I_{0q1}, from 9(a) and 9(b), the following is obtained:

$$V_{0p} = x\left(Z_{0m}I_{0p2} + Z_{0s1}I_{0p1}\right) + V_{0se} + \frac{R_f}{(1-x)}\left(I_{0p1} - k_0 I_{0p2}\right) + \frac{AV_{0inj}}{(1-x)(Z_{0s1} - Z_{0m})} + \frac{Z_{0SSSC}I_{0p1}A}{(1-x)(Z_{0s1} - Z_{0m})} \tag{10}$$

Where: $k_0 = (Z_{0s2} - Z_{0m})/(Z_{0s} - Z_{0m})$ (11)

For the parallel lines with identical parameters, $k_l = k_0$=1.
For an a-g fault, the boundary condition is:

$$V_{0se} + V_{1se} + V_{2se} = 0 \tag{12}$$

From above, the voltage at the relay point can be derived as:

$$V_p = x\left(Z_{1s1}I_{p1} + (Z_{0s1} - Z_{1s1})I_{0p1} + Z_{0m}I_{0p2}\right) + \frac{R_f}{(1-x)}\left(I_{p1} - k_1 I_{p2} + (k_1 - k_0)I_{0p2}\right) + \Delta V \tag{13}$$

Where:

$$V_{0p1} + V_{1p1} + V_{2p1} = V_p \tag{14}$$
$$I_{0p1} + I_{1p1} + I_{2p1} = I_{p1}$$
$$I_{0p2} + I_{1p2} + I_{2p2} = I_{p2}$$

And:

$$\Delta V = \frac{A}{(1-x)Z_{1s1}}(Z_{1SSSC}I_{p1} + V_q + I_{0p1}\left(\frac{Z_{0SSSC}Z_{1s1}}{(Z_{0s1} - Z_{0m})} - Z_{1SSSC}\right) + V_{0q}\left(\frac{1}{(Z_{0s1} - Z_{0m})} - 1\right)) \tag{15}$$

In the transmission system without SSSC, for a single phase-to-ground fault, the apparent impedance of distance relay can be calculated using the following equation:

$$Z = \frac{V_p}{I_{p1} + (\frac{Z_{0s1} - Z_{1s1}}{Z_{1s1}})I_{0p1}} = \frac{V_p}{I_{Relay}} \tag{16}$$

If this traditional distance relay is applied to the transmission system with SSSC, the apparent impedance seen by this relay can be expressed as:

$$Z = xZ_{1s1} + xZ_{0m}\frac{I_{0p2}}{I_{Relay}} + \frac{R_f}{(1-x)I_{Relay}}\left(I_{p1} - k_1 I_{p2} + (k_1 - k_0)I_{0p2}\right) + \Delta Z \tag{17}$$

Where:

$$\Delta Z = \frac{1}{I_{Relay}}\left(V_q + V_{0q}\left(\frac{Z_{1s1}}{(Z_{0s1})} - 1\right)\right) + \frac{R_f}{(1-x)Z_{1s1}I_{Relay}}\left(V_q + V_{0q}\left(\frac{Z_{1s1}}{(Z_{0s1})} - 1\right)\right) \tag{18}$$

From (18) it can be observed that if the SSSC is placed at the relaying point on one of the circuits of the double circuit transmission line, the apparent impedance seen by the relay for a single-line-to-ground fault is influenced by the SSSC.

B. SSSC at the Relaying Point

When a single phase-to-ground fault occurs and the distance is X from the relay point or SSSC, similar to the aforementioned method ΔZ is calculated:

(19)

$$\Delta Z = Z_{1SSSC} + (Z_{0SSSC} - Z_{1SSSC} - Z_{0m})\frac{I_{0p1}}{I_{p1}} + \frac{V_{0q}}{I_{p1}} + \frac{R_f}{Z_{1s1}(1-x)}\left(Z_{1SSSC} + \frac{V_q}{I_{p1}} - \frac{V_{0q}}{I_{p1}} - \frac{Z_{1SSSC}I_{0p1}}{I_{p1}}\right)$$

IV. Relay Modeling

A procedure for designing a fault impedance estimation algorithm for distance protection is discussed in this section. Positive, negative and zero sequence networks of the system experiencing the fault from the relay located near bus P and various shunt fault conditions were used to derive the performance (20) where in (20) and the coefficients S_1, S_2, and S_0, are listed in Table 1 (a=-0.5+j0.866 and a^2=-0.5-j0.866) [14]. Also note that e_r is the error term in the estimation of the distance due to fault resistance and SSSC.

(20)

$$X = \frac{S_1V_{1p} + S_2V_{2p} + S_0V_{0p}}{S_1I_{1p1}Z_{1s1} + S_2I_{2p1}Z_{1s1} + S_0(I_{0p1}Z_{0s1} + I_{0p2}Z_{0m})} + e_r$$

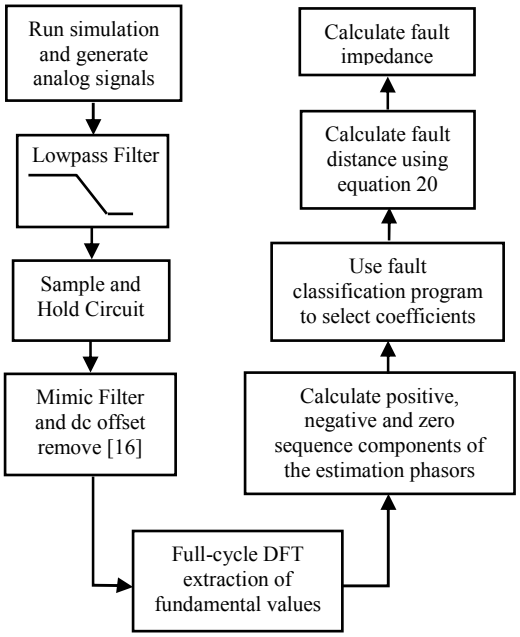

Fig. 5. Basic modules of distance relaying.

TABLE I
FAULT TYPE COEFFICIENT OF EQUATION 20

Fault type	*Equation 20*		
	S_1	S_2	S_0
A-G	1	1	1
B-G	a^2	a	1
A-B	1	$-a$	0
A-B-G	a	0	-1

A digital distance relaying algorithm proposed by the authors use the phasor estimates, sequence components of phasors and fault classification scheme [15], before calculating fault distance where its basic modules are shown Fig. 5. The measured voltages and currents at the relay point are sampled at 32 samples per cycle.

V. Simulation Results

In the following parts, the location of fault, the type of fault, the location of SSSC and the setting of SSSC will be considered.

A. Single Phase-to-Ground Fault

Fig. 6 depict the apparent impedance seen by the distance relay for an A-G fault at a fault distance 150 km from the relaying point.

As shown in figure 6, when the SSSC is not used, the relay recognizes the impedance value correctly and then enters to the zone 1. When the SSSC is used, the relay is overreached and failed to act because the impedance is considered beyond its real place. To show the effect of different working states of SSSC, the impedance values calculated by the relay for different states of SSSC is shown.

As mentioned earlier, SSSC compensates for the voltage independent of the line current in the form of series voltage [1]. As shown in Fig. 7 after the fault occurrence, the compensating voltage injected by SSSC increases; however it's clear from Fig. 8 that the amplitude of the injected voltage is remained fixed on 0.1.

It should be noticed that after A-G fault the injected voltage to phase a from SSSC leads the current of phase a by 90 degrees. This is completely different from the previous state of SSSC i.e. whether the injected voltage by the SSSC leads or lags the current, the injected voltage to the defect phase would lead the current in phase (figures 7, 9). This phenomena is due to decrease in the line reactance which is independent of the prior state of the SSSC. If the SSSC was in the inductive compensating mode the value of the apparent part of the impedance calculated by the relay would be more than the state in which the SSSC was in capacitive compensating mode (Fig. 11).

To study the coverage of the mho characteristic, faults at different positions have been studied, and the apparent reactance and resistance as a function of the fault location are shown in Figs. 11 and 12, respectively. It is apparent that when the fault is on the left side of SSSC (i.e., < 100 Km), the apparent impedance seen by the distance relay is almost the

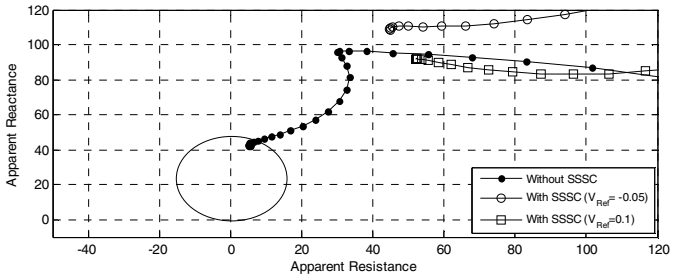

Fig. 6. Impedance seen by the Mho relay (A-G fault and with/without SSSC and different SSSC setting and SSSC at the middle point (fault distance =150 km)).

very same as that for the system without SSSC; however, when the fault is on the right side of SSSC, both the apparent resistance and reactance of the system with SSSC are larger than for the system without SSSC; this phenomena can be explained by the ΔZ.

The effect of negative, positive and zero sequence of the injected voltage by the SSSC on is shown in Fig. 10. As shown in the figure the zero element of the injected voltage has the dominant effect (relation 18). It is also can be seen when the SSSC is in the beginning of the line ,where the relay is located; the apparent impedance seen by the relay is affected by the SSSC. Note that for the distances more than 100 km, the apparent impedance for both of the SSSC places is the same. It can be concluded that when the SSSC is placed in the middle of the line, the relay can not recognize the faults occurred in the distances beyond 100 km and, when the relay is in the beginning it fails for all faults.

B. Two Phase-to-Ground Fault

In this section the SSSC is supposed to be located in the place of relay. There is a simple justification for this choice. As shown in the previous section, when the SSSC is located in the middle of the line its impact on the calculated impedance, by the relay, for left-sided faults is negligible. On the other hand, for the right-sided faults the equivalent circuit is the same with when the SSSC is located in where the relay is located (figure 1a). For the 2-phase to ground errors it is different. The apparent resistance and reactance calculated by A-B-G element of the relay to the different places of errors are shown in figures 13 and 14, respectively. The other controversial elements of the replay are also included in these figures. It is shown that when the place in where the faults occurred is beyond 65 km, the A-B-G element of the relay can not recognize the fault (Fig. 15). In other words the place seems to be away from its place. However, this problem is not

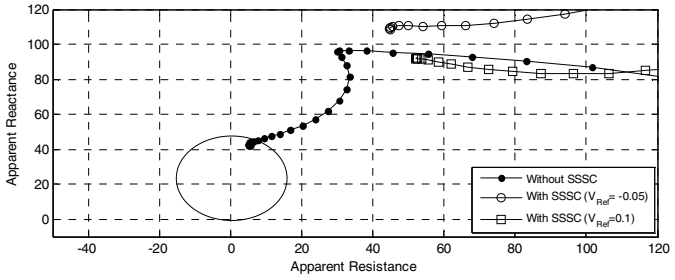

Fig. 6. Impedance seen by the Mho relay (A-G fault and with/without SSSC and different SSSC setting and SSSC at the middle point (fault distance =150 km)).

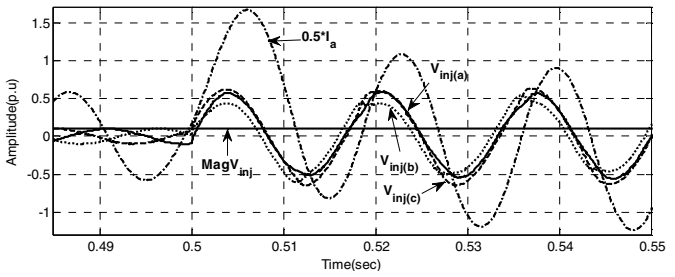

Fig. 7. 48-pulse converter output three phase voltage and line current (A-G fault and SSSC operating in capacitive mode and SSSC at the midpoint (fault distance =150 km)).

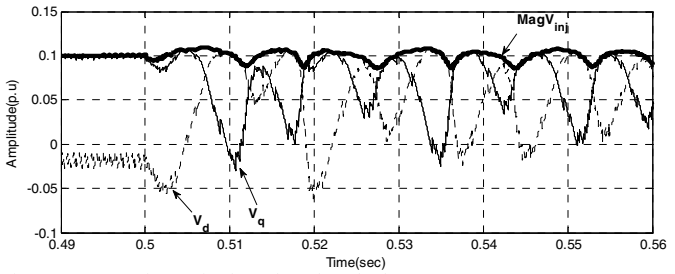

Fig. 8. Output of magnitude and angle calculator system

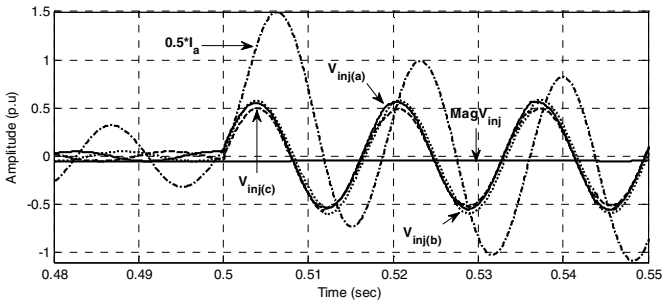

Fig. 9. 48-pulse converter output three phase voltage and line current (A-G fault and SSSC operating in inductive mode and SSSC at the midpoint (fault distance =150 km)).

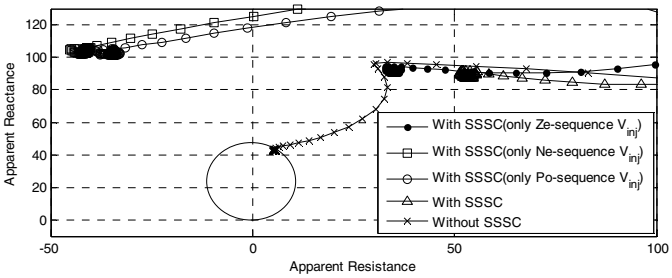

Fig. 10. Impedance seen by the Mho relay (A-G fault and with/without SSSC and SSSC at the midpoit and SSSC operating in capacitive mode (fault distance =150 km)).

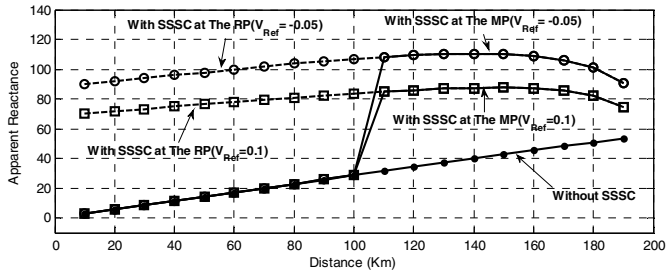

Fig. 11. Apparent reactance with different fault location (a-g fault and with/without SSSC and different SSSC setting).

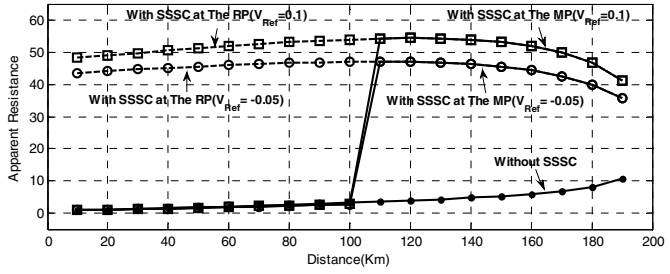

Fig. 12. Apparent resistance with different fault location (a-g fault and with/without SSSC and different SSSC setting).

a serious one compared to the single-phase fault. It should be noted that the apparent impedance reactance calculated by A-B-G element of relay is out of the region. In contrast with the single-phase to ground fault, the 2-phase faults can be recognized by the other elements of the relay. A-G element of the relay can recognize the faults occurred until 115 km. B-G element recognizes the faults until 95 km. A-B element recognizes the faults until 165 km. The A-B-G element covers the faults up to 165 km and therefore, the relay fails to act correctly for the faults occurred between 156 to 165 km. For example, the calculated impedance by the relay for the fault occurred at 162 is shown Fig. 16. It can be also observed that the apparent reactance calculated by A-B element in the specified region is very close to the one calculated by A-B-G element when the SSSC is not used.

When SSSC is in inductive reactance compensating mode the distance covered by all the aforementioned elements of the relay decreases because in this case the increase in apparent impedance calculated by the relay is more than the one in capacitive reactance compensating mode (figures 17, 18).

A-B-G element recognizes the faults until 47 km, A-G element up to 80 km, B-G element up to 74 km and A-B element up to 143 km.

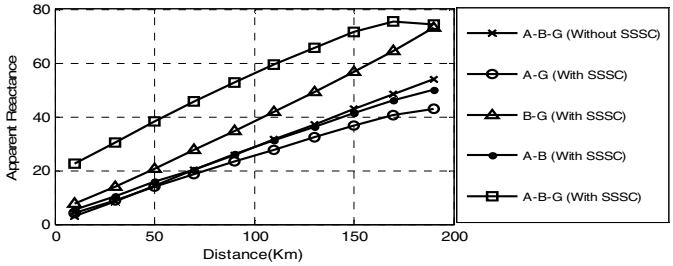

Fig. 13. Apparent reactance seen by different relay elements with different fault location during A-B-G fault (SSSC at the relaying point and SSSC operating in capacitive mode).

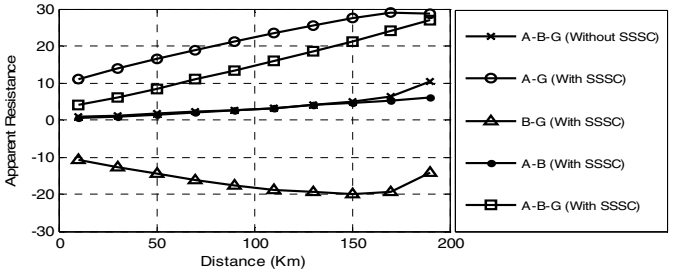

Fig. 14. Apparent resistance seen by different relay elements with different fault location during A-B-G fault (SSSC at the relaying point and SSSC operating in capacitive mode).

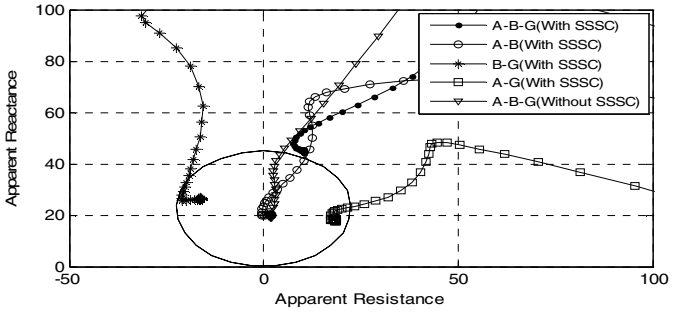

Fig. 15. Apparent impedance seen by different relay elements during A-B-G fault (SSSC at the relaying point and SSSC operating in capacitive mode (fault distance= 67 km)).

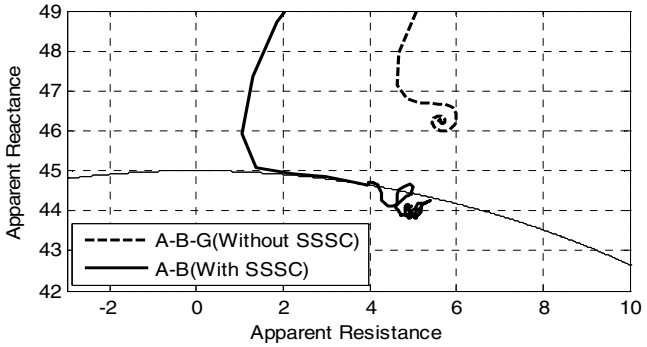

Fig. 16. Apparent impedance seen by different relay elements during A-B-G fault (SSSC at the relaying point and SSSC operating in capacitive mode (fault distance= 162 km)).

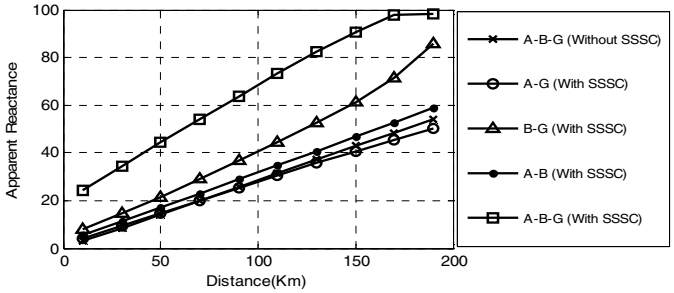

Fig. 17. Apparent reactance seen by different relay elements with different fault location during A-B-G fault (SSSC at the relaying point and SSSC operating in inductive mode).

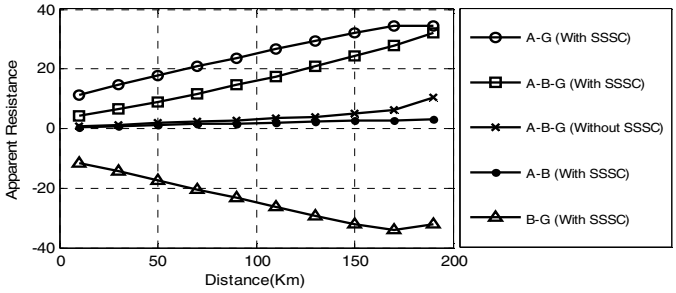

Fig. 18. Apparent resistance seen by different relay elements with different fault location during A-B-G fault (SSSC at the relaying point and SSSC operating in inductive mode).

VI. Appendix

The 200 km, 500 kV double-circuit transmission line considered for computer simulation has the following data:
Positive sequence impedance of line=0.0201+j 0.2868 Ω/km
Zero sequence impedance of line=0.1064+j 0.8670 Ω/km
Parameters for sources at P and Q are:
Z_{1sp}=1.7431+j 19.424 Ω, Z_{1sq}=0.8716+j 9.7120 Ω
Z_{0sp}=2.6147+j 4.886 Ω, Z_{0sq}=1.3074+j 2.4430 Ω
Load angle between sources=20°

VII. References

[1] N. G. Hingorani and L. Gyugyi, *Understanding FACTS Concepts and Technology of Flexible AC Transmission Systems*, New York: IEEE Press, 2000.

[2] Kalyan K. Sen, "SSSC – Static Synchronous Static Compensator: Theory, Modeling, and Applications," *IEEE Trans. Power Delivery*, vol. 13, no. 1, pp. 241-246, Jan. 1998.

[3] , *Power System Protection*, Vol. 2. Edited by The Electricity Training Association.

[4] K. El-Arroudi, G. Joos, and D. T. McGillis, "Operation of impedance protection relays with the STATCOM," *IEEE Trans. Power Delivery*, vol. 17, no. 2, pp. 381–387, Apr. 2002.
[5] T. S. Sidhu, R. K. Varma, Pradeep Kumar Gangadharan
[6] P. K. Dash, A. K. Pradhan, G. Panda, and A. C. Liew, "Adaptive relay setting for flexible AC transmission systems (FACTS)," *IEEE Trans. Power Delivery*, vol. 15, no. 1, pp. 38–43, Jan. 2000.
[7] M. Khederzadeh, and T. S. Sidhu, "Impact of TCSC on the protection of transmission Lines," *IEEE Trans. Power Delivery*, vol. 21, no. 1, pp. 80–87, Jan. 2006.
[8] M. Khederzadeh, "The impact of FACTS device on digital multifunctional protective relays," in Proc. *IEEE/PES Transmission and Distribution Conf. and Exhib. 2002*: *Asia Pacific*, vol. 3, Oct. 6–10, 2002, pp. 2043–2048.
[9] P. K. Dash, A. K. Pradhan, G. Panda, and A. C. Liew, "Digital protection of power transmission lines in the presence of series connected FACTS devise," in *Proc. IEEE Power Engineering Soc. Winter Meeting*, vol. 3, Jan. 23–27, 2000, pp. 1967–1972.
[10] D. Novosel, A. Phadke, M. M. Saha, and S. Lindahl, "Problems and solutions for microprocessor protection of series compensated lines," *Proc. Inst. Elect. Eng. Conf. Developments Power System Protection*, pp. 18–23, Mar. 25–27, 1997.
[11] X. Zhou, H. Wang, R. K. Aggarwal, and P. Beaumont, "Performance evaluation of a distance relay as applied to a transmission system with UPFC," *IEEE Trans. Power Delivery*, vol. 21, no. 3, pp. 1137–1147, Jul. 2006.
[12] M. S. El-Moursi and A. M. Sharaf, "Novel Controllers for the 48-Pulse VSC STATCOM and SSSC for Voltage Regulation and Reactive Power Compensation," *IEEE Trans. Power Syst*, vol. 20, no. 4, pp. 1985–1997, Nov. 2005.
[13] Y. Liao, and S. Elangovan, "Digital distance relaying algorithm for first-zone protection for parallel transmission lines," *IEE Proc.-Gener. Transm. Distrib*., vol. 145, no. 5, pp. 531-536, Sep. 1998.
[14] D. L. Waikar, S. Elangovan, and A. C. Liew, "Fault impedance estimation algorithm for digital distance relaying," *IEEE Trans. Power Delivery*, vol. 9, no. 3, pp. 1375–1383, Jul. 1994.
[15] M. S. Sachdev, and S. R. Kolla, "A polyphase digital distance relay," *Transactions of the Engineering and Operating Division, Canadian Electrical Association*, vol. 26, part 4, no 87-SP-170, pp. 1-19, Mar. 1987.
[16] G. Benmouyal, "Removal of DC-offset in current waveforms using digital mimic filtering," *IEEE Trans. Power Delivery*, vol. 10, no. 2, pp. 621–630, Apr. 1995.